DFT Modeling of Chemical Vapor Deposition of GaN from Organogallium Precursors. 2. Structures of the Oligomers and Thermodynamics of the Association Processes†

Alexey Y. Timoshkin*

Inorganic Chemistry Group, Department of Chemistry, St. Petersburg State University, University Pr. 2, Old Peterhof, 198904, Russia

Holger F. Bettinger‡ and Henry F. Schaefer III§

Center for Computational Quantum Chemistry, University of Georgia, Athens, Georgia 30602

Received: July 3, 2000; In Final Form: November 28, 2000

The thermochemistry of association reactions of organogallium precursors for the GaN chemical vapor deposition (CVD) is studied. Geometries, relative energies, and vibrational frequencies of ring and cluster compounds $[RGaNR']_n$, $[R_2GaNR'_2]_m$, ($n = 2-4, 6$; $m = 2-3$; R, R′ = H, CH_3) are obtained at the hybrid Hartree−Fock/density functional level of theory (B3LYP/pVDZ). Formation of the $[RGaNR']_4$ tetramer and $[RGaNR']_6$ hexamer species is thermodynamically favorable in the gas phase at temperatures up to 720 K (R = H, R′ = CH_3) and 920−940 K (R = H, CH_3, R′ = H). The thermodynamic analysis of the major gas-phase reactions indicates that association processes might play a key role in the GaN CVD under low-temperature−high-pressure conditions.

Introduction

Doped gallium nitride is a prospective material for controlled color light-emitting diodes for lighting and display applications. One of the most common ways of GaN fabrication is metal organic vapor phase epitaxy (MOVPE) of trimethylgallium $Ga(CH_3)_3$ (TMG) and ammonia. Several reactor schemes have been used to reduce "parasitic" gas phase reactions between the donor and acceptor components in early investigations of the GaN CVD process.[1] Such efforts have been stimulated by the assumption that the CVD of GaN at high temperatures is similar to the CVD mechanism of the higher homologue GaAs, which is known from experiment and theory to involve radical and surface reactions.

The formation of GaAs from different precursors has been studied extensively by electronic structure theory.[2−6] Whereas Bock et al.[2] considered only simple GaH_x and AsH_x ($x = 1-3$) species in their early work, gallane, arsine, trimethylgallium $Ga(CH_3)_3$ (TMG), and their adducts have been studied up to the CCSD level of theory by Graves and Scuseria.[3] The latter group found that exothermic formation of the H_3AsTMG adduct proceeds without an activation barrier. A wide range of methyl, chloro, and fluoro gallanes and their adducts with AsH_3, as well as adducts of gallane with $As(CH_3)_xH_{3-x}$ ($x = 1, 2$) have been investigated at the MP4(SDTQ) level of theory.[4] The higher stability of halide complexes with arsine has been explained on the basis of a bonding interaction between the halogen and As atoms.

Bock and Trachtman[5] studied the GaAs CVD mechanism in more detail by looking at possible CH_4 elimination reactions from *trans*-$(CH_3)HGaAsH(CH_3)$. Besides the two α-elimination reaction paths from either the Ga or As centers, a transition state for the interfragment CH_4 elimination (barrier of 58 kcal mol^{-1}) could be located at the MP2/HUZSP**//RHF/HUZSP* level of theory. The bond dissociation energies of *trans*-$CH_3HGaAsHCH_3$ increase in the order As−C < Ga−As < As−H < Ga−C < Ga−H. The Ga−C bond dissociation energy (293 kJ mol^{-1}) is 50 kJ mol^{-1} larger than that of the As−C bond (243 kJ mol^{-1}). Therefore, Bock et al.[5] concluded that the 2-methylpropene observed experimentally in the thermal decomposition of $(t\text{-Bu})_2GaAs(t\text{-Bu})_2$ is produced via β-elimination from the Ga center rather than from any radical reaction in the gas phase:

$$(t\text{-Bu})_2GaAs(t\text{-Bu})_2 = (t\text{-Bu})HGaAs(t\text{-Bu})_2 + CH_2{=}C(CH_3)_2$$

A detailed thermodynamic analysis of the gas-phase radical reactions between TMG and AsH_3 involving seven major elementary gas-phase reactions was presented in 1988 by Tirtowidjojo and Pollard.[7] These seven gas-phase reactions were investigated in 1995 by Trachtman et al.,[6] who found that the radical mechanism plays an important role at high temperatures. The thermal decomposition of TMG proceeds as a homogeneous gas-phase reaction at 1000 K, but surface catalysis is required at lower temperatures. This theoretical prediction is in agreement with experimental results on the photodissociation of TMG adsorbed on the surface of GaAs. The photodissociation is a one-photon process and occurs on the surface of GaAs.[8]

It is generally accepted that the precursors used for CVD of GaAs form the weak adducts $Ga(CH_3)_3AsH_3$ or $GaH_3As(CH_3)_3$. It is assumed that CVD from organogallium compounds involves dissociation of the weak Ga−As bond, followed by Ga−C and As−C bond breaking. Whereas only dissociation products are believed to exist in the gas phase at high temperatures, additional

† Part 1: DFT Modeling of Chemical Vapor Deposition of GaN from Organogallium Precursors. 1. Thermodynamics of Elimination Reactions. *J. Phys. Chem. A* **2001**, *105*, 3240.

* Corresponding author. E-mail: alex@dux.ru.

‡ E-mail: hfsiii@arches.uga.edu.

§ Present address: Department of Chemistry MS 60, PO Box 1892, Rice University, Houston, TX 77098-1892.

10.1021/jp002380g CCC: $20.00
Published on Web 03/06/2001

intermediates are formed on the GaAs surface at low temperatures. The operation of a radical mechanism is also supported by the presence of C_2H_6 in products of $Ga(CH_3)_3AsH_3$ thermal decomposition.[9]

Theoretical research on the CVD of GaN from organogallium precursors is far less extensive than for GaAs. Because of lack of data, many experimental studies have assumed that the CVD of GaN at high temperatures is similar to the dissociative and radical mechanism described above for GaAs.[10] Indeed, the observation of C_2H_4 and C_2H_6 traces during $Ga(CH_3)_3$-NH_3 MOCVD supports this assumption.[1,11] However, there are several indications that the GaN CVD mechanism differs from that of GaAs significantly. GaN films, obtained at 950 °C in Ar or N_2 carrier gas, contained intermediate products like $(CH_3)_{3-x}GaNH_{3-x}$.[12] Thon and Kuech observed formation of a $[(CH_3)_2GaNH_2]_x$ species under MOCVD conditions "with most probably $x = 3$".[1] Recently, Kuech and co-workers mentioned that "the exact chemistry involved in the MOVPE of GaN, has not been reported".[13] Supposedly,[14] the CVD process involves the following steps:

$$(CH_3)_3Ga + NH_3 \rightarrow (CH_3)_3GaNH_3$$

$$(CH_3)_3GaNH_3 \rightarrow {}^1/_n[(CH_3)_2GaNH_2]_n + CH_4$$

$$[(CH_3)_2GaNH_2]_n \rightarrow {}^1/_m[(CH_3)GaNH]_m + CH_4$$

It was shown in our previous work that the Ga−N bond dissociation energy is much higher than that for Ga−As (138 and 40 kJ mol^{-1} for $GaCl_3NH_3$ and $GaCl_3AsH_3$, respectively).[15] Therefore, preserving the metal-pnictide bond via cluster formation in the gas phase maybe more important for Ga−N than for Ga−As systems. The experimentally observed particle formation in the gas phase during the CVD of AlN indicates association processes.[16,17] The theoretical thermochemical study of the Cl_3AlNH_3 adduct showed that in this system oligomerization to clusters as large as $(ClAlNH)_6$ is thermodynamically favorable in the gas phase.[18] Solid AlN is formed presumably via cluster association in the gas phase, rather than by a radical mechanism. It should be noted that HCl elimination from the Cl_3AlNH_3 adduct causes an increase of the Al−N bond strength (420 kJ mol^{-1} for Cl_2AlNH_2 compared to 149 kJ mol^{-1} for Cl_3AlNH_3).[18] The same trend, however at lower bond energies, is predicted for the Ga−As bond dissociation energy: 249 kJ mol^{-1} for $(CH_3)HGaAsH(CH_3)$, but only 52 kJ mol^{-1} for the $(CH_3)H_2GaAsH_2(CH_3)$ precursor with larger Ga and As coordination numbers.[5] Because the Ga−N bond dissociation energy is much higher compared to Ga−As [378 kJ mol^{-1} for $(CH_3)GaNH_2$ and 76 kJ mol^{-1} for $(CH_3)_3GaNH_3$], association processes should be more favorable for GaN than for GaAs systems.

The notion that association processes are important for Ga−N systems is further supported by experimental results. The Ga_2N_2 rings of $[R_2GaN{=}CR'R'']_2$ and $[Me_2GaNRR']_2$ compounds (R, R′, R″ = Me, Ph) were found in mass-spectroscopy studies to be highly stable in the gas phase.[19−21] The major fragmentation processes are the terminal Ga−C and N−C bond cleavages. It is also known that mixing TMG with NH_3 immediately leads to the TMG-NH_3 adduct, which evolves 1 mol of CH_4 accompanied by $[(CH_3)_2GaNH_2]_3$ trimer formation when heated above 120 °C.[22] In addition, Koplitz and co-workers found in the recent study of the laser-assisted reaction of TMG with ammonia not only formation of TMG:NH_3 and TMG:NH_2 adducts, but also "higher mass GaN-containing species."[23] Lee and Stringfellow[24] investigated the MOVPE of GaN from TMG and 1,1-dimethylhydrazine. These authors found that both compounds form an adduct which loses CH_4 at 250 °C forming presumably $Me_2Ga{-}NHNMe_2$, but no evidence for breaking of the Ga−N bond at higher temperatures is observed during the CVD of GaN. Miehr et al. studied the CVD of GaN from an organogallium azide.[25] Best results were obtained using the nitrogen-rich single molecule precursor in the absence of carrier gases, whereas NH_3 carrier gas caused oligomerization of the precursor. A very recent mass-spectrometric study revealed dimer formation in the gas phase during GaN MOCVD at temperatures below 1000 K.[26]

Of course, experimental CVD processes are rather controlled by kinetic factors. Therefore, nonthermal activation channels, such as photon- and electron-initiated chemistry at surfaces, are widely used.[27] However, the "thermodynamic analysis is noteworthy in understanding and optimizing the selective epitaxial growth processes",[28] and in many cases the film composition is determined by the thermodynamics. The total pressure P in the system defines the mechanism of the CVD process. Only when the probability of gas-phase collisions is negligible ($P < 10^{-4}$ Torr) the precursor decompositions become strictly heterogeneous.[28] Because the standard CVD apparatus use higher pressures, it seems reasonable to consider association reactions in the gas phase.

Since thermodynamic properties of many gas-phase organogallium precursors and possible intermediates are not known, we investigate computationally structural and thermodynamic aspects of CVD of GaN from organogallium precursors. Whereas monomer donor−acceptor compounds and their dissociation products have been considered in Part I of this series, the present report focuses on the association products: small rings and clusters $[RGaNR']_n$, $[R_2GaNR'_2]_m$, $n = 2{-}4,6$; $m = 2{-}3$; R, R′ = H, CH_3. Vibrational spectra of all compounds investigated are given in the Supporting Material section and may help in the experimental identification of possible intermediates in the GaN CVD process. We present enthalpies, entropies and Gibbs energies of the major processes in the gas phase. We do not consider TMG and NH_3 decay processes as they are relatively well understood today and do not play a significant role in the MOCVD process under low-temperature−high-pressure conditions.

Computational Details

All computations were performed using the Gaussian 94 program package.[29] All geometries were fully optimized using self-consistent-field (SCF) and density functional theory (DFT). The three-parameter exchange functional of Becke[30] with the gradient-corrected correlation functional of Lee, Yang, and Parr[31] (B3LYP) was used for the DFT studies. The polarized valence double-ζ (pVDZ) basis set of Ahlrichs and co-workers[32] was used throughout. These basis sets are contracted in the following way: H (4s, 1p) → [2s, 1p]; C (7s, 4p, 1d) → [3s, 2p, 1d]; N (7s, 4p, 1d) → [3s, 2p, 1d]; Ga (14s, 10p, 6d) → [5s, 4p, 3d]. The effective core potential (ECP) basis set of Hay and Wadt,[33] augmented by d and p polarization functions (LANL2DZP) was also employed in preliminary computations. All stationary points of the potential energy surface (PES) were characterized by analytic evaluation of second derivatives, with the exception of structures computed with the LANL2DZP basis set, for which second derivatives were evaluated by finite differences of analytic first derivatives.

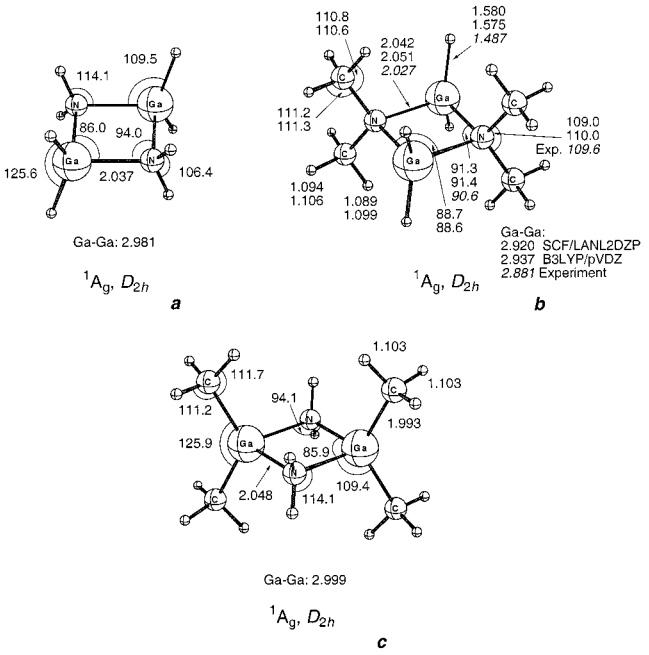

Figure 1. Geometries of tetra-coordinated dimer compounds: $[H_2GaNH_2]_2$ (a), $[H_2GaN(CH_3)_2]_2$ (b), and $[(CH_3)_2GaNH_2]_2$ (c) at the B3LYP/pVDZ (a and c) and SCF/LANL2DZP and B3LYP/pVDZ (b) levels of theory. Bond lengths are in Å, bond angles in degrees.

Results and Discussion

I. Oligomer Compounds. *A. Dimer Species $[R_2GaNR'_2]_2$ (R, R′ = H, CH_3) with Tetracoordinated Ga and N Centers.* $[H_2GaNH_2]_2$. While trimeric cyclotrigallazane $[H_2GaNH_2]_3$ has been synthesized and extensively investigated very recently,[34] the dimer $[H_2GaNH_2]_2$ is still unknown. The computed minimum structure of this unknown compound has D_{2h} symmetry with a planar Ga_2N_2 core (Figure 1a).

$[H_2GaNMe_2]_2$. This white crystalline compound has been studied by Downs and co-workers.[35] The dimeric structure of the compound has been observed in the gas phase and in benzene solution.[36] Baxter et al.[35] were able to fit their gas-phase electron diffraction data with a planar Ga_2N_2 ring and a $[C_2NGaH_2]_2$ skeleton with D_{2h} symmetry. Positions of hydrogen atoms in CH_3 groups have been fixed with a twisting angle of 20°. Our optimized D_{2h} symmetry structure with a planar Ga_2N_2 core is given in Figure 1b. The bond distances are slightly longer than the experimental values, but this difference is usually observed at the B3LYP/pVDZ level of theory. Bond angles within the Ga_2N_2 core agree well with experiment, and so do the computed vibrational spectra (see Supporting Information).[35]

$[Me_2GaNH_2]_2$. In contrast to $[H_2GaNMe_2]_2$, its $[Me_2GaNH_2]_2$ isomer is not known experimentally, but there exists a trimer $[Me_2GaNH_2]_3$ of the Me_2GaNH_2 unit. However, the optimized geometry of the D_{2h} symmetry dimer is close to that of its $[H_2GaNMe_2]_2$ isomer and is given in the Figure 1c. Note that the $[Me_2GaNH_2]_2$ isomer lies 225 kJ mol^{-1} lower in energy than $[H_2GaNMe_2]_2$, confirming the trend of the preferable Me-Ga and N−H orientation of substituents, which was found for the monomer species.[63]

It is well-known that the degree of association in oligomer species strongly depends on the steric demand of the substituents: more bulky ligands result in a lower degree of association.[37,38] From experimental observations it is concluded that the steric influence of substituents is more pronounced if these are bound to the smaller nitrogen atom. Indeed, substitution of the NH_2 group by NMe_2 renders association more difficult: whereas the trimers $[Me_2GaNH_2]_3$ and $[H_2GaNH_2]_3$ are known, $[H_2GaNMe_2]$ was found to exist only as a dimer. There are many successful reports on the synthesis and identification of dimeric $[R_2GaNR'_2]_2$ compounds with different substituents R and R′.[36,39−48] $[Me_2GaNH(t\text{-}Bu)]_2$ was synthesized and characterized in 1992 by two groups working independently.[45,46] The important structural data of these compounds are summarized in Table 1.

The GaNGa angles are larger than the NGaN angles in compounds having Ga_2N_2 rings, in agreement with findings for the analogous aluminum species.[18] This trend (Table 1) is well-known for group 13−15 compounds.[37,38] The Ga−N bond distance is increased by 0.217 (H,H), 0.205 (H,Me) and 0.217 (Me,H) Å compared to the monomer $R_2GaNR'_2$ molecules. Here and later on in this paper the notation (H, Me) indicates that the first substituent (H) is attached to the Ga center, and the second one (Me) to the nitrogen center, i.e., H_2GaNMe_2. The terminal Ga−R and N−R′ bonds are elongated by about 0.007−0.016 Å due to dimerization, and a significant change of RGaN and GaNR′ bond angles is observed due to removal of the quasi-planar structure of $R_2GaNR'_2$ monomers. Despite these structural reorganizations and the strain due to the small ring size, the energy of formation of two additional GaN bonds compensates all unfavorable structural changes, making the enthalpy of the dimerization process

$$R_2GaNR'_2 = {}^1/_2[R_2GaNR'_2]_2$$

exothermic by −97 (H,H), −76 (H, Me) and −91 (Me, H) kJ mol^{-1}. Entropy changes are unfavorable by 93, 94, and 105 J mol^{-1} K^{-1} for (H, H), (H, Me), and (Me, H) orientation of substituents, respectively.

B. Trimer Species $[R_2GaNR'_2]_3$ (R, R′ = H, CH_3) with Tetracoordinated Ga and N Centers. $[H_2GaNH_2]_3$. This trimeric cyclogallazane has been studied extensively recently.[34,49,50] It was found to be a suitable precursor for GaN deposition by Gladfelter and co-workers,[34] and its decomposition in solution was further investigated in a recent report.[49] This compound can be produced from H_3GaNMe_3 and ammonia and eventually converted into GaN.[34,50] On the basis of X-ray structural data of $[H_2GaNH_2]_3$ and neutron powder diffraction of $[D_2GaND_2]_3$, Gladfelter and co-workers established a chair conformation of cyclotrigallazane in the solid state. However, they found that the twist-boat conformation of $[H_2GaNH_2]_3$ is more stable (by 11 kJ mol^{-1}) than the chair conformation at the MP2/VDZ level of theory. Therefore, we do not consider chair conformations in the present work. The boat conformation of C_s symmetry is a transition state (Hessian index one) and lies only 1 kJ mol^{-1} higher in energy than the C_2 symmetric twist-boat minimum (Figure 2a).

$[H_2GaNMe_2]_3$. Geometric parameters for this unknown compound are presented in Figure 2b and vibrational frequencies are reported in the Supporting Information.

$[Me_2GaNH_2]_3$. $[Me_2GaNH_2]_3$ is easily produced when the source Me_3GaNH_3 adduct is heated above 120 °C.[14] Our optimized structure is given in Figure 1c. Similar to its hydrogen analogue, the twist-boat structure of C_2 symmetry was found to be a minimum on the PES. The $[Me_2GaNH_2]_3$ species exists in the "twisted sofa" form in the solid state with the smallest torsion angle for consecutive Ga−N−Ga−N atoms being only 2.7°.[14] However, the smallest torsion angle between consecutive Ga−N−Ga−N atoms for our computed (gas-phase) structure is 26°, but this difference may be caused by intermolecular

TABLE 1: Selected Experimental and Theoretical Geometries for Oligomer Compounds

CN	Compound	R(Ga−N)	Ga−N−Ga	N−Ga−N	method	ref
4	$[H_2GaNH_2]_2$	2.037	94.0	86.0	B3LYP/pVDZ	present
	$[H_2GaNMe_2]_2$	2.027	90.6	89.4	electron diffraction	35
	$[H_2GaNMe_2]_2$	2.051	91.4	88.6	B3LYP/pVDZ	present
	$[Me_2GaNH_2]_2$	2.048	94.1	85.9	B3LYP/pVDZ	present
	$[Me_2GaNHDipp]_2$	2.025	94.2	83.6	X-ray	46a
	$[Me_2GaNH(1\text{-}Ad)]_2$	2.031	94.7	85.3	X-ray	46a
	$[Me_2GaNH(1\text{-}Ad)]_2$	2.030	94.8	85.2	X-ray	47
	$[Me_2GaNHPh]_2$	2.039	93.6	86.4	X-ray	46a
	$[t\text{-}Bu_2GaNHt\text{-}Bu]_2$	2.065	98.3	81.7	X-ray	41
	$[Cy_2GaNHPh]_2$	2.038	95.6	84.4	X-ray	42a
	$[Cy_2GaNHt\text{-}Bu]_2$	2.01	95.4	84.6	X-ray	42a
	$[t\text{-}Bu_2GaNHPh]_2$	2.018−2.103	96.5	83.5	X-ray	42b
	$[Me_2GaNHt\text{-}Bu]_2$	2.012	95.3	84.8	X-ray	42c
	$[Me_2GaNHt\text{-}Bu]_2$	2.023	94.7	85.3	X-ray	45a
	$[Et_2GaN(H)NPh_2]_2$	2.042−2.070	93.4−94.6	85.8−86.2	X-ray	39b
	$[(Me_2N)N_3GaNMe_2]_2$	1.992−1.998	92.5	87.5	X-ray	39a
	$[(Me_2N)_2GaNMe_2]_2$	2.005−2.021	92.3	87.7	X-ray	46b
	$[(t\text{-}Bu(H)N)_2GaN(H)t\text{-}Bu]_2$	2.008	94.8	81.6	X-ray	40b
	$[Me_2GaN(H)NPh_2]_2$	2.043	93.15	86.75	X-ray	45b
	$[Me_2GaN(H)SiEt_3]_2$	2.029	91.9	88.2	X-ray	45c
	$[Me_2GaN(CH_2Ph)_2]_2$	2.044	89.9	90.0	X-ray	43
	$[Me_2GaN(CH_2CH_2)_2NMe]_2$	2.032	92.4	87.6	X-ray	43
	$[Me_2GaN(i\text{-}Pr)SnMe_3]_2$	2.034	90.7	89.3	X-ray	44
	$[Me_2GaN(C_6H_{11})_2]_2$	2.068	89.5	90.5	X-ray	44
	$[Et_2GaN(i\text{-}Bu)_2]_2$	2.035−2.061	88.2−88.5	86.8−87.9	X-ray	44
	$[Et_2GaN(C_6H_{11})_2]_2$	2.049−2.086	86.8−88.2	87.1−88.0	X-ray	44
	$[PhMe_2CCH_2GaNHPh]_2$	2.037−2.082	93.8−94.7	86.2−85.3	X-ray	48a
	$[PhMe_2CCH_2GaNH(n\text{-}Pr)]_2$	2.013−2.029	93.3	86.7	X-ray	48b
	$[(t\text{-}Bu)_2GaN(H)t\text{-}Bu]_2$	2.018−2.103	96.5	83.5	X-ray	42d
	$[H_2GaNH_2]_3$	1.972−1.987	116.9−117.3	99.9−100.6	X-ray, neutron diffraction	34
	$[H_2GaNH_2]_3$	2.01	123.7	102.6	SCF/ECP	34
	$[H_2GaNH_2]_3$	2.026−2.034	117.6−119.5	99.4−100.2	B3LYP/pVDZ	present
	$[H_2GaNMe_2]_3$	2.037−2.055	113.6−115.3	108.2−108.9	B3LYP/pVDZ	present
	$[Me_2GaNH_2]_3$	1.93−2.05	119.5−125.3	93.8−101.3	X-ray	22
	$[Me_2GaNH_2]_3$	2.038−2.041	121.8−123.2	99.6−100.8	B3LYP/pVDZ	present
	$[HGaNH]_4$	2.001	92.3	87.7	B3LYP/pVDZ	present
	$[HGaNMe]_4$	2.007	91.1	88.9	B3LYP/pVDZ	present
	$[MeGaN(C_6F_5)]_4$	1.995−2.017	85.9−88.8	91.5−94.0	X-ray	52
	$[(C_6F_5)HNGa(MesGa)_3(\mu_3\text{-}NC_6F_5)]_4$	2.001−2.023	91−95	85−89	X-ray	53
	$[MeGaNt\text{-}Bu]_4$	1.984−1.999	90.6−91.4	88.6−89.2	X-ray	54
	$[MeGaNSiMe_3]_4$	1.981−1.994	89.6−90.3	89.6−90.4	X-ray	55
	$[MeGaNH]_4$	2.005	92.3	87.6	B3LYP/pVDZ	present
	$[HGaNH]_6$[a]	1.966−1.968	126.3−126.8	113.4−113−7	B3LYP/pVDZ	present
		2.051	91.5	88.15		
	$[HGaNMe]_6$[a]	1.974−1.976	123.1−123.6	116.6−117.0	B3LYP/pVDZ	present
		2.053	90.2	89.7		
	$[MeGaN(4\text{-}C_6H_4F)]_6$[a]	1.967−1.971	129.5	114.1	X-ray	57a
		2.033	90.35	89.35		
	$[MeGaNi\text{-}Bu]_6$[a]	1.937−1.955	125.7	113.8	X-ray	57b
		2.067	88.6−89.1	90.6−90.1		
	$[MeGaNH]_6$[a]	1.969−1.970	126.9−127.1	113.1−113.4	B3LYP/pVDZ	present
		2.056	91.45	88.15		
3	$[HGaNH]_2$	1.864	91.9	88.1	B3LYP/pVDZ	present
	$[HGaNMe]_2$	1.867−1.875	90.8	89.2	B3LYP/pVDZ	present
	$[MeGaNH]_2$	1.868	92.1	87.9	B3LYP/pVDZ	present
	$[HGaNH]_3$	1.814	126.0	114.0	SCF/ECP	61
	$[HGaNH]_3$	1.844	126.5	113.5	B3LYP/pVDZ	present
	$[HGaNMe]_3$	1.848−1.856	122.5	117.5	B3LYP/pVDZ	present
	$[MeGaNH]_3$	1.848−1.851	127.1	112.9	B3LYP/pVDZ	present

[a] For the hexamer compounds, data in the first row refer to the six-membered ring, and data in the second row refer to the four-membered ring.

interactions in the crystal. Our predicted vibrational frequencies (Supporting Information) are close to experimental IR data obtained in an argon matrix.[14]

The computed enthalpies of the dimerization-trimerization reactions

$$^1/_2[R_2GaNR'_2]_2 = {}^1/_3[R_2GaNR'_2]_3$$

are very low: −7, +2, and −4 kJ mol^{-1} for the (H,H), (H,Me), and (Me,H) orientation of substituents, respectively. Note that the formation of the trimer is favorable for $[H_2GaNH_2]_2$ and $[Me_2GaNH_2]_2$, but unfavorable for $[H_2GaNMe_2]_2$, in excellent agreement with experimental observations: there are two stable trimers $[H_2GaNH_2]_3$[34] and $[Me_2GaNH_2]_3$[14] and one stable dimer $[H_2GaNMe_2]_2$.[35] Since the energy of the reorganization processes is very small, additional interactions may play a dominant role in solution and thus a dimer−trimer equilibrium may exist in solutions for all (H,H), (H,Me) and (Me,H) dimer or trimer molecules.

C. Dimer Species $[RGaNR']_2$ (R, R′ = H, CH_3) with Tricoordinated Ga and N Centers. Further RR′ elimination from

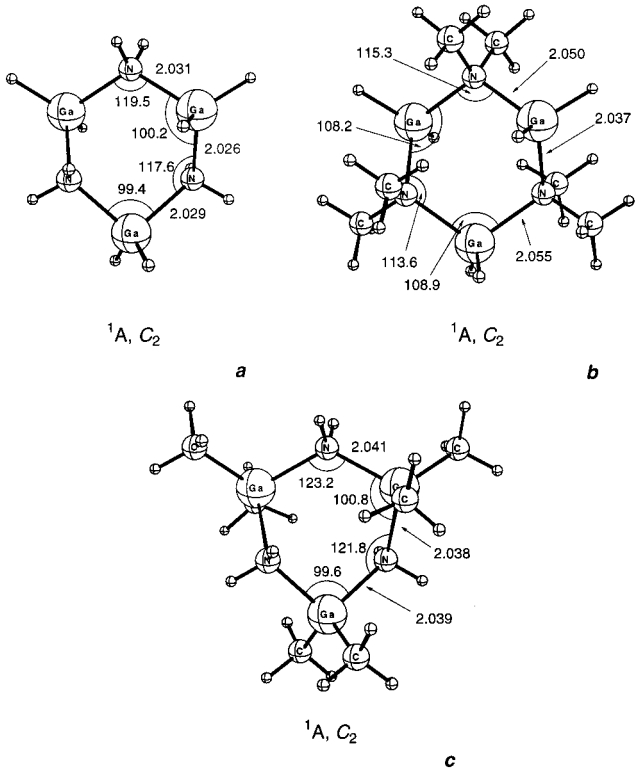

Figure 2. Geometries of tetra-coordinated trimer compounds: $[H_2GaNH_2]_3$ (a), $[H_2GaN(CH_3)_2]_3$ (b), and $[(CH_3)_2GaNH_2]_3$ (c) at the B3LYP/pVDZ level of theory. Bond lengths are in Å, bond angles in degrees.

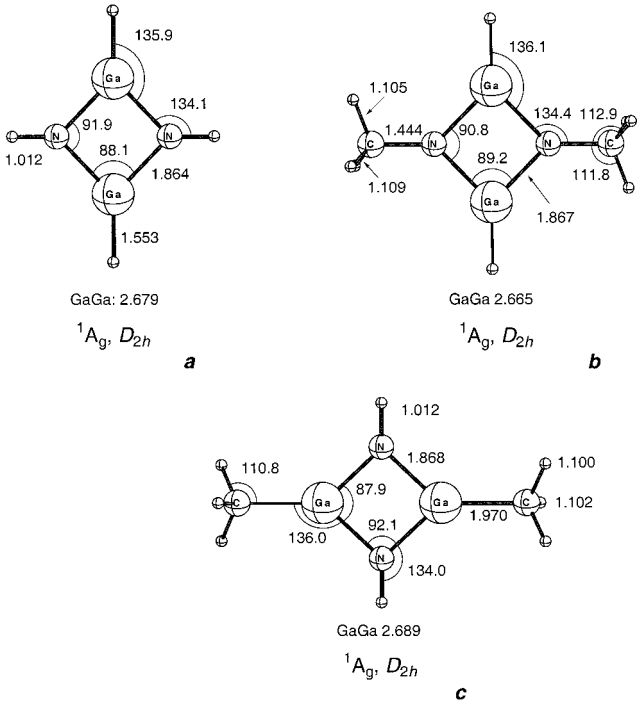

Figure 3. Geometries of dimer compounds: $[HGaNH]_2$ (a), $[HGaN(CH_3)]_2$ (b), and $[(CH_3)GaNH]_2$ (c) at the B3LYP/pVDZ level of theory. Bond lengths are in Å, bond angles in degrees.

the dimer and trimer compounds with tetracoordinated Ga and N may result in formation of oligomer species with tricoordinated Ga and N centers. None of the compounds investigated here have been synthesized, most probably due to high tendency for polymerization of such species, which favor infinite lattice formation.[49]

$[HGaNH]_2$. This dimeric compound has D_{2h} symmetry (Figure 3a). The Ga−N bond length (1.864 Å) is significantly (by 8.5%) shorter than in the corresponding $[H_2GaNH_2]_2$ dimer (2.037 Å), while the terminal Ga−H and N−H distances expectedly show less variation (1.3% and 1%, respectively). Thus, the strong dependence of the Ga−N bond length on the Ga and N coordination numbers, found already for the monomers,[63] is also observed for the cluster species.

$[HGaNMe]_2$ and $[MeGaNH]_2$. The highest possible point group for these compounds is C_{2h}, but the C_2 axis can be oriented in two different ways: (1) C_2 axis perpendicular to the ring plane and through the center of the Ga_2N_2 ring and (2) H−N−N−H or H−Ga−Ga−H atoms lying on the C_2 axis. From these two cases, a large number of lower symmetry structures (C_{2v}, C_i, and C_2 point groups) can be derived. Preliminary studies at the SCF/LANL2DZP level of theory showed that each of the optimized structures of C_{2h}, C_{2v}, and C_i symmetry have two imaginary vibrational frequencies. However, both $[HGaNMe]_2$ and $[MeGaNH]_2$ are minima with C_{2h} symmetry at the B3LYP/pVDZ level. But the two isomers differ in the orientation of the methyl groups. Whereas the $[HGaNMe]_2$ isomer prefers the conformation where one H atom of each methyl group lies in the Ga_2N_2 ring plane [C_2 axis orientation (1)], the C_2 axis orientation (2) is found for $[MeGaNH]_2$ (Figure 3b,c). In each instance, the other possible C_{2h} conformers are saddle points with one small imaginary (7i cm^{-1}) and one small real (2 cm^{-1}) vibrational frequency. The energy difference between the minima and saddle points of $[HGaNMe]_2$ or $[MeGaNH]_2$ is no more than 0.02 kJ mol^{-1}, and the bond lengths stay constant within 0.001 Å, and bond angles within 0.1°. We conclude that, as in the case of TMG,[63] the rotation of the methyl groups in dimers $[MeGaNH]_2$ and $[HGaNMe]_2$ is essentially free.

D. Trimer Species [RGaNR′]$_3$ (R, R′ = H, CH$_3$) with Tricoordinated Ga and N Centers. $[HGaNH]_3$. This compound has D_{3h} point group with a planar Ga_3N_3 core (Figure 4a). Earlier on, "gallazene" was studied theoretically by Matsunaga and Gordon[51] together with other benzene analogues.

$[HGaNMe]_3$ and $[MeGaNH]_3$. We obtained a C_{3v} symmetry minimum for $[MeGaNH]_3$ (Figure 4c) with an orientation of the methyl groups similar to the one found in the dimer $[MeGaNH]_2$. The lowest vibrational frequencies are 15 cm^{-1} (A_2) and 17 cm^{-1} (E). Geometry optimization of $[HGaNMe]_3$ in C_{3h} symmetry converged to a structure (Figure 4b) which has two low vibrational frequencies, 21 cm^{-1} (A″) and 32 cm^{-1} (E″). Ga−N bond lengths are shortened by 0.02 Å compared to the corresponding dimer compounds, indicating stronger bonding in the six-membered ring. Indeed, enthalpies for the reorganization reaction dimer = trimer are exothermic (Table 3).

E. Tetramer Species [RGaNR′]$_4$ (R, R′ = H, CH$_3$) with Tetracoordinated Ga and N Centers. In contrast to aluminum analogues with the Al_4N_4 core, which have been known since 1962,[51] compounds with a Ga_4N_4 cube were only discovered in 1993, when the synthesis and crystal structure of $[MeGaN(C_6F_5)]_4$ had been reported.[53] Thereafter, more compounds with Ga_4N_4 core structures have been prepared and identified: $(C_6F_5)HNGa(MesGa)_3(\mu_3\text{-}NC_6F_5)_4$,[54] $[MeGaNR]_4$ (R = *i*-Pr, *t*-Bu),[55] and $[MeGaNSiMe_3]_4$.[56] Note that three compounds have methyl substituents at the Ga center. All these compounds have a cubic skeleton with Ga−N bond distances in the range of 1.972−2.039 Å, and Ga···Ga distances between 2.797 and 2.900 Å. The T_d symmetry geometries of $[HGaNH]_4$, $[HGaN(CH_3)]_4$, and $[(CH_3)GaNH]_4$ are presented in Figure 5a−c. The GaNGaN atoms forming the face of the cube are not coplanar, but the

TABLE 2: Selected Characteristics of Oligomer Compounds $[R_xGaNR'_x]_n$, Standard Enthalpies $\Delta H^{ass}_{(298)}$ and Entropies $\Delta S^{ass}_{(298)}$ for the Association Process $R_xGaNR'_x = {}^1/_n[R_xGaNR'_x]_n$ and Standard Enthalpies $\Delta H^{elim}_{(298)}$ and Entropies $\Delta S^{elim}_{(298)}$ for the Process $R_3Ga + NR'_3 = {}^1/_n[R_xGaNR'_x]_n + (3-x)RR'$: All Results Are from the B3LYP/pVDZ Level of Theory

n	x	R,R′	$S^0_{(298)}$, J mol^{-1} K^{-1}	μ, D	$\Delta H^{ass}_{(298)}$, kJ mol^{-1}	$\Delta S^{ass}_{(298)}$, J mol^{-1} K^{-1}	$\Delta H^{elim}_{(298)}$, kJ mol^{-1}	$\Delta S^{elim}_{(298)}$, J mol^{-1} K^{-1}
		H,H	341	0	−96.6	−92.8	−144.6	−109.8
	2	H,CH_3	459.6	0	−76.1	−94.1	−188.2	−90.4
2		CH_3,H	517	0	−91.2	−105.4	−174.0	−144.0
		H,H	320.2	0	−206.8	−91.0	−17.5	10.5
	1	H,CH_3	423.0	0	−196.4	−85.5	−157.2	77.7
		CH_3,H	440.6	0	−200.6	−89.5	−94.2	4.1
		H,H	448.2	1.38	−103.3	−113.9	−151.3	−130.9
	2	H,CH_3	579.6	1.00	−73.7	−130.7	−185.8	−126.9
3		CH_3,H	717.8	0.94	−95.2	−124.6	−178.0	−163.2
		H,H	389.1	0	−265.3	−121.4	−76.0	−19.9
	1	H,CH_3	533.6	0	−241.4	−119.1	−202.1	44.0
		CH_3,H	574.4	0.05	−255.9	−118.3	−149.5	−24.7
		H,H	397.9	0	−306.1	−151.6	−116.8	−50.2
4	1	H,CH_3	534.1	0	−286.3	−163.5	−247.1	−0.3
		CH_3,H	580.2	0	−298.0	−164.7	−191.6	−71.2
		H,H	524.9	0	−326.4	−163.6	−137.1	−62.2
6	1	H,CH_3	721.9	0	−299.4	−176.7	−260.2	−3.2
		CH_3,H	807.3	0	−316.9	−175.2	−210.5	−81.7

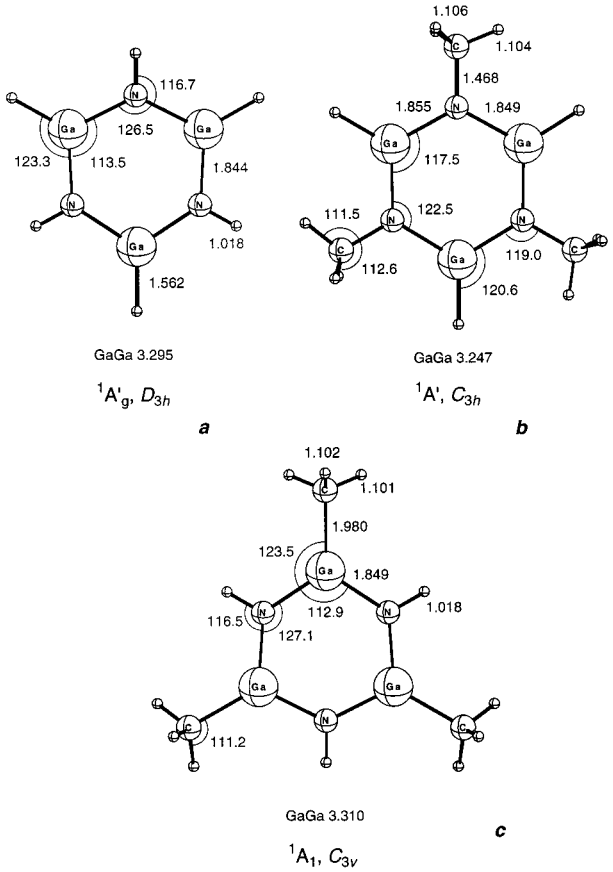

Figure 4. Geometries of trimer compounds: $[HGaNH]_3$ (a), $[HGaN(CH_3)]_3$ (b), and $[(CH_3)GaNH]_3$ (c) at the B3LYP/pVDZ level of theory. Bond lengths are in Å, bond angles in degrees.

distortion angle θ from planarity is 2.3°, 1.1°, and 2.4°, for (H, H), (H, Me), and (Me, H) species, respectively. The computed Ga−N bond lengths (2.001, 2.007, and 2.005 Å), and Ga···Ga distances (2.886, 2.865, and 2.892 Å) are in the range of those reported for the synthesized compounds, and the theoretical NGaN and GaNGa angles also fit well into the 85.9−89.2° and 90.6−94.0° experimental margins. The Ga−C bond length in $[MeGaNH]_4$ is computed to be 1.977 Å, which is longer than in $[MeGaN(C_6F_5)]_4$ (1.926−1.933 Å), and in $[MeGaNSiMe_3]_4$ (1.944−1.953 Å), but agree well with the Ga−C distance

TABLE 3: Standard Enthalpies ΔH_{298} (kJ mol^{-1}) for Oligomerization Reactions. B3LYP/pVDZ Level of Theory

		n			
reaction	(R,R′)	2	3	4	6[a]
${}^1/_{n-1}[R_2GaNR'_2]_{n-1} =$	(H,H)	−97	−7		
${}^1/_n[R_2GaNR'_2]_n$	(H,Me)	−76	+2		
	(Me,H)	−91	−4		
${}^1/_{n-1}[RGaNR']_{n-1} =$	(H,H)	−207	−59	−41	−20
${}^1/_n[RGaNR']_n$	(H,Me)	−196	−45	−45	−13
	(Me,H)	−201	−55	−42	−19

[a] Values are given for the reaction ${}^1/_4[RGaNR']_4 = {}^1/_6[RGaNR']_6$.

reported for [MeGaN*t*-Bu]$_4$ (1.965−1.996 Å). It should be noted that $[MeGaNR]_4$ cube compounds (R = *t*-Bu, *i*-Pr) have been produced by the following route:

$$Me_3GaNH_2R \rightarrow [Me_2GaNHR]_2 \rightarrow [MeGaNR]_4$$

At the last stage, thermolysis of dimeric $[Me_2GaNHR]_2$ amidogallanes was observed at 250−260 °C. Formation of such $[MeGaNR]_4$ species during the CVD process via a similar reaction scheme should be possible and will be discussed in section III.

F. Hexamer Species [RGaNR′]$_6$ (R, R′ = H, CH$_3$) with Tetracoordinated Ga and N Centers. The first experimentally known hexamer iminogallane $[MeGaN(4\text{-}C_6H_4F)]_6$ (**1**) has been structurally characterized in 1997 by Schnitter et al.,[57a] and the second hexamer imidogallane [MeGaN*i*-Bu]$_6$ (**2**) was reported in 1999 by Weidlein and co-workers.[57b] Both compounds have S_6 point group symmetry in the solid state due to the bulkiness of the 4-fluorophenyl and *iso*-butyl substituents. Optimized structures of hexamer species are presented in Figure 6. Our theoretical data for $[MeGaNH]_6$ agrees well with experimental results: calculated Ga−N (six-membered ring), Ga−N (four-membered ring), and Ga−C distances are 1.970, 2.056, and 1.984 Å, respectively. The experimental lengths of these bonds are 1.969(5), 2.033(4) and 1.943(5) Å for (**1**) and 1.937−1.955(2), 2.067(3), and 1.956(3) Å for (**2**), respectively. Predicted Ga−N distances in the six-membered ring are 0.086 Å shorter than those compared to Ga−N distances in four-membered ring, in good agreement with the experimental differences of 0.066 Å (**1**) and 0.112−0.13 Å (**2**). In the mass spectrum of $[MeGaN(4\text{-}C_6H_4F)]_6$ hexamer (28%), tetramer (10%), dimer (100%), and monomer (10%) units have been

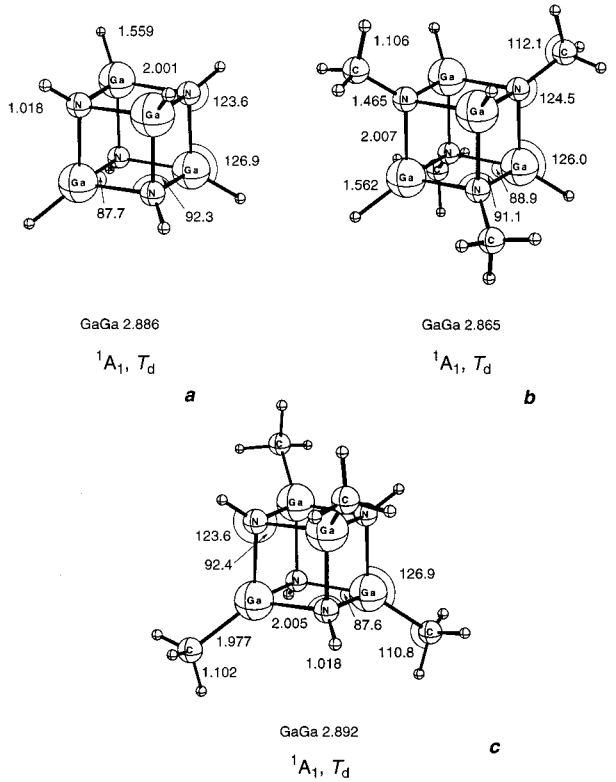

Figure 5. Geometries of tetramer compounds: $[HGaNH]_4$ (a), $[HGaN(CH_3)]_4$ (b), and $[(CH_3)GaNH]_4$ (c) at the B3LYP/pVDZ level of theory. Bond lengths are in Å, bond angles in degrees.

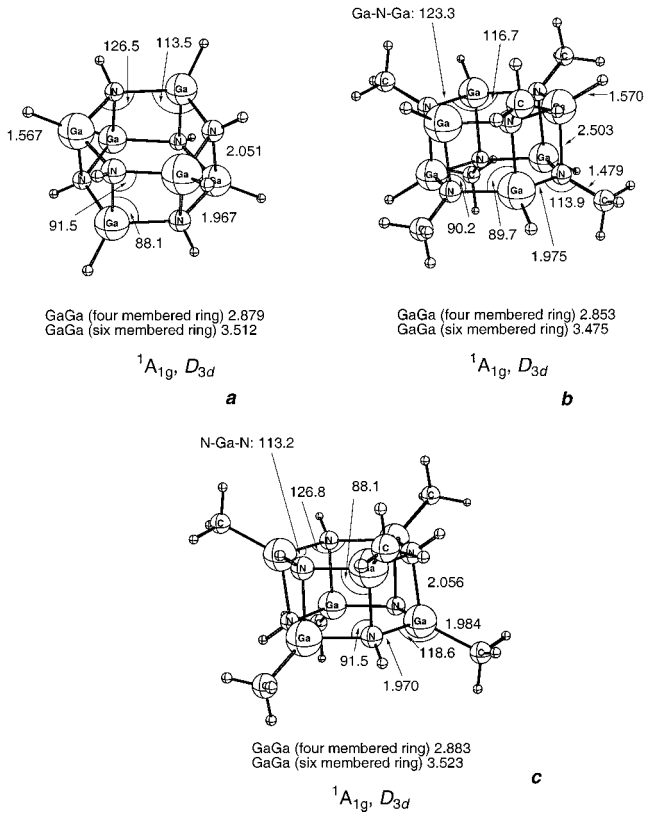

Figure 6. Geometries of hexamer compounds: $[HGaNH]_6$ (a), $[HGaN(CH_3)]_6$ (b), and $[(CH_3)GaNH]_6$ (c) at the B3LYP/pVDZ level of theory. Bond lengths are in Å, bond angles in degrees.

observed.[57a] Note that no trimer units have been observed under mass spectroscopy (MS) conditions despite the longer Ga−N distances between six-membered rings. This may reflect the fact that six Ga−N bonds need to be broken to produce two timers, while only four Ga−N bonds need to dissociate to yield the dimer, monomer or tetramer. The enthalpies of dissociation of the hexamers into two trimers $[RGaNR']_6 = 2\,[RGaNR']_3$ [366, 349, and 336 kJ mol^{-1} for the (H, H), (H, Me), and (Me, H), respectively] are by 46, 91, and 58 kJ mol^{-1} *higher* than the enthalpies of dissociation into tetramer and dimer $[RGaNR']_6 = [RGaNR']_4 + [RGaNR']_2$. Thus, the dissociation products observed by mass spectroscopy are more stable thermodynamically. All hexamer compounds are predicted to be more stable than tetramers (Table 3). The similar stability of hexamer compounds in the Cl−Al−N−H system was attributed to decreased Al−Al repulsion compared to tetramers.[18]

II. Vibrational Frequencies of Compounds. Unscaled vibrational frequencies and infrared intensities for all 18 distinct compounds are available as Supporting Information. The performance of the B3LYP/pVDZ method was tested on molecules for which experimental gas-phase or matrix isolation IR and Raman spectra are available: NH_3,[58] $Ga(CH_3)_3$,[59] $H_3GaN(CH_3)_3$,[60,61] $(CH_3)_3GaN(CH_3)_3$,[62] $[H_2GaN(CH_3)_2]_2$,[35] and $[(CH_3)_2GaNH_2]_3$[14] (total of 70 experimental frequencies). There is a good correlation between observed and calculated vibrational frequencies:

$$\nu_{obs} = 0.9469\,\omega_{calc} + 33.3\ cm^{-1},$$

correlation coefficient 0.9995.

We recommend the use of this correlation to scale predicted vibational frequencies for the cluster compounds (Table 1s) in order to compare predicted values with experimental data.

III. Discussion: Thermodynamics of CVD Processes. A general scheme of GaN CVD processes as obtained from our investigation of their thermodynamics is given in Figure 7. There are two major pathways for CVD of gallium nitride: the dissociation pathway (formation of GaR_x, and NR'_x radicals and their reactions on the surface) and the association pathway (gas phase $[R_xGaNR'_x]_n$ cluster generation and their nucleation). The thermodynamic characteristics of dissociation and elimination processes of monomer compounds have been reported in the previous paper.[63]

Enthalpies of the major association processes are given in Table 3. The oligomerization reactions of $R_xGaNR'_x$ monomer compounds are highly exothermic for all substituents R and R′, with association enthalpies being larger for $x = 1$ than for $x = 2$. The dimer−trimer equilibrium reaction $^1/_2[R_xGaNR'_x]_2 = {}^1/_3[R_xGaNR'_x]_3$ is exothermic by 45−60 kJ mol^{-1} in the case of $x = 1$, while the enthalpy of this reaction is close to zero for $x = 2$. Therefore, we can predict that further association of the saturated $[R_2GaNR'_2]_n$ species is hardly favored by enthalpy, but strongly disfavored by entropy. Thus, further association of amidogallanes is expected to be unfavorable. In contrast, for unsaturated $[RGaNR']_n$ oligomers, further association is strongly favorable energetically: the oligomerization reaction

$$^1/_{n-1}[RGaNR']_{n-1} = {}^1/_n[RGaNR']_n$$

is exothermic by −45 to −60 kJ mol^{-1} for $n = 3$ and about −40 kJ mol^{-1} for $n = 4$. Enthalpies of the cubic tetramer to hexamer conversion

$$^1/_4[RGaNR']_4 = {}^1/_6[RGaNR']_6$$

are also exothermic by −13 to −20 kJ mol^{-1}. Thus, further

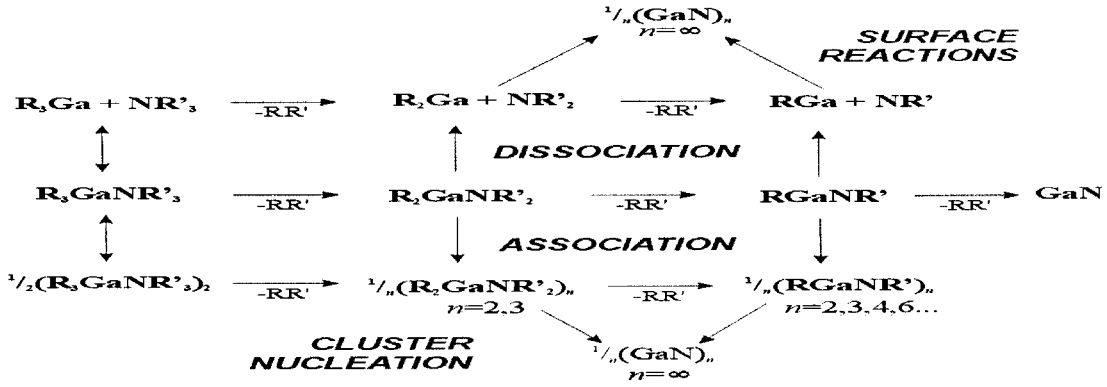

Figure 7. Schematic of the GaN CVD process.

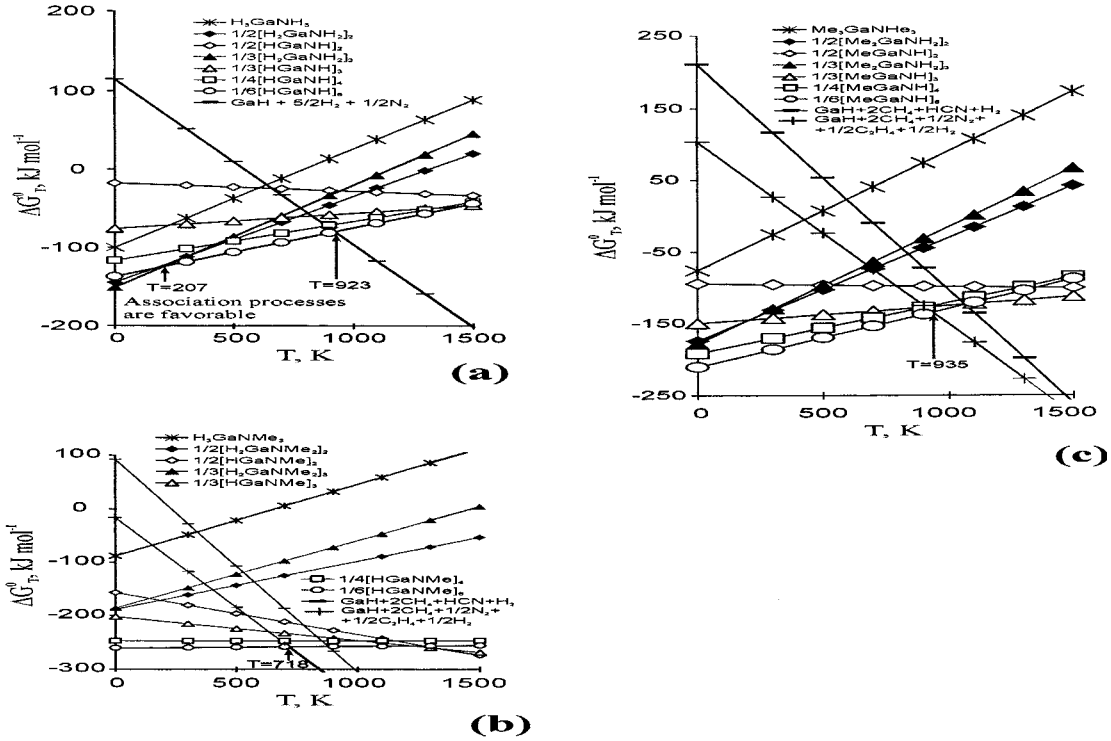

Figure 8. Gibbs energy−temperature dependence for the elimination reactions $R_3Ga + NR'_3 = {}^1/_n[R_xGaNR'_x]_n + (3-x)RR'$ and dissociation reactions 1−5 as obtained at the B3LYP/pVDZ level of theory: R═R′ = H (a), R═H, R′ = Me (b), R = Me, R′ = H (c).

association of imidogallanes is expected to be favorable energetically.

For the thermodynamic analysis of possible gas-phase reactions, Gibbs energy-temperature diagrams are used. In Figure 8, Gibbs energies are presented for the gas-phase elimination reactions

$$R_3Ga + NR'_3 = {}^1/_n[R_xGaNR'_x]_n + (3-x)RR'$$

for the (H,H) (a), (H,Me) (b), and (Me,H) (c) species. In all cases the original stoichiometry of the adduct compounds is preserved by setting the R_3Ga/NR'_3 ratio to 1. The process with the lowest Gibbs energy leads to the thermodynamically most favorable products. From Figure 8a one can clearly see that for the (H,H) system the trimeric cyclotrigallazane $[R_2GaNR'_2]_3$ is predicted to be the most stable Ga-N-H containing species at low temperatures (up to 207 K), in agreement with the experimental observations of Gladfelter and co-workers.[34,49] As the temperature increases above 207 K, the $[HGaNH]_6$ hexameric cluster becomes the thermodynamically most stable gas-phase molecule. The analogous hexameric clusters $[RGaNR']_6$ are also the most stable in (H, Me) and (Me, H) systems (Figure 8b,c). Other imidogallanes considered (tetramer, trimer, and dimer) are less stable but the difference in their stability decreases with increasing temperature since the entropy factor favors dissociation processes. The existence of the trimeric intermediate $[Me_2GaNH_2]_3$ was proposed based on an IR spectroscopy study,[1] but our thermodynamic analysis shows (Figure 8c) that this trimeric amidogallane is not the most stable gas-phase molecule. The intermediate trimer may form the most stable hexamer by dimerization of two trimeric rings, a process favorable by both enthalpy and entropy:

$$2\,[Me_2GaNH_2]_3 = [Me_2GaNH_2]_6 + 6\,CH_4$$

With further temperature increase, dissociation yielding small molecules like H_2 and Ga−H start to compete with cluster formation. In the present study we considered only one dissociation reaction for (H, H) systems (eq 1) and two dissociation processes for (H, Me) and (Me, H) systems (eqs 2−5):

$$H_3GaNH_3 = GaH + {}^5/_2H_2 + {}^1/_2N_2 \quad (1)$$

$$(CH_3)_3GaNH_3 = GaH + 2CH_4 + HCN + H_2 \quad (2)$$

$$(CH_3)_3GaNH_3 = GaH + 2CH_4 + {}^1/_2N_2 + {}^1/_2C_2H_4 + {}^1/_2H_2 \quad (3)$$

$$H_3GaN(CH_3)_3 = GaH + 2CH_4 + HCN + H_2 \quad (4)$$

$$H_3GaN(CH_3)_3 = GaH + 2CH_4 + {}^1/_2N_2 + {}^1/_2C_2H_4 + {}^1/_2H_2 \quad (5)$$

We expect simple species like GaH, HCN, N_2, H_2, CH_4, and C_2H_4 to be the most stable molecules in the gas phase at high temperatures. The thermodynamic characteristics of processes leading to their formation from the corresponding donor−acceptor complexes are presented in Table 4. All these processes are strongly endothermic, but the entropy will have an overwhelming effect on the Gibbs energy at increasing temperatures. The temperatures at which formation of small gas phase species becomes thermodynamically favorable over $[RGaNR']_6$ cluster formation are 923, 718, and 935 K, for the (H, H), (H, Me) and (Me, H) systems, respectively (Figure 8). These temperatures are the upper limit of the operation of association reactions with regard to the competitive dissociation processes. The much lower temperature for the (H, Me) system arises from the inherently lower stability of Ga−H and N−CH_3 orientation of substituents (vide supra). From our thermodynamic analysis we conclude that the association pathway (Figure 7) of the GaN CVD process from TMG and ammonia is predominant from normal conditions until temperatures up to 940 K (Figure 8c), which are working temperatures for commercial GaN production. Our prediction is in excellent agreement with very recent mass-spectrometric observations, carried out for masses up to 240 amu. It has been shown that dimeric forms $[(CH_3)_4Ga_2(NH_2)_2]$, $[(CH_3)_3Ga_2(NH_2)_2]$, and $[(CH_3)_3Ga_2(NH_2)]$ are present in the gas phase in the 300−1000 K temperature range.[26] No dimeric species have been observed above 1000 K. The calculated temperatures at which dissociation of amidogallane dimer species into monomers becomes favorable are 1041, 808, and 865 K for $[H_2GaNH_2]_2$, $[H_2GaNMe_2]_3$, and $[Me_2GaNH_2]_2$, respectively. These temperatures set the limit of operation of association reactions with respect to formation of monomeric species with Ga−N bond. Although oligomerization of imidogallanes is thermodynamically favorable even at higher temperatures, dimeric amidogallanes are the least stable species in the oligomerization chain, and thus oligomers will be less important at higher temperatures. On the other hand, association products should dominate the gas phase at lower temperatures if thermodynamic equilibrium were achieved.

To avoid thermodynamically favorable association processes, higher temperatures and low reactor pressure conditions are needed. On the other hand, high thermodynamic stability of the gas-phase clusters makes them promising precursors for the stoichiometry-controlled CVD processes.

Conclusions

The results obtained in the present paper suggest that under the experimental conditions of the GaN deposition process small clusters of Ga−N compounds may play a key role as intermediates. Some of the species considered here, such as dimeric $[H_2GaNMe_2]_2$ and trimeric $[Me_2GaNH_2]_3$ are known to exist in the gas phase and even have previously been isolated and structurally characterized in the solid state and in nonaqueous solutions. However, until recently their presence in the GaN MOCVD process was speculative, as a direct observation has not been made. Despite the suggestions of Thon and Kuech[1] in 1996 that such compounds, particularly the trimer $[Me_2GaNH_2]_3$, may play some role in MOCVD of GaN, their experimental setup "would not be capable to determine these high molecular weight species." Our thermochemical analyses suggest that the whole series of $[R_xGaNR'_x]_n$ compounds may exist in the gas phase. In their recent paper on the laser-assisted MOCVD of GaN under high pressure-low temperature (well below room temperature) conditions, Koplitz and co-workers[23] identified the formation of a new TMG-NH_2 adduct, "and diverse, higher mass GaN-containing species". According to our calculations, hexameric $[MeGaNH]_6$ cluster is the most stable gas-phase molecule in the $GaMe_3-NH_3$ system below 935 K. Very recently dimeric clusters have also been observed in the gas phase in the temperature interval 300−1000K.[26] However, experimental setup was able to detect masses up to 240[26] or 300[23] amu, and from the obtained data it is not clear if the largest mass observed at 217 amu [ascribed to $Me_3HGa_2(NH_2)NH^+$][23] and 234 amu [ascribed to $Me_4Ga_2(NH_2)_2^+$][26] result from the dimer or from some heavier GaN containing species. It is very important to note that the relative MS intensity of the cluster compounds in the gas phase is increasing under laser irradiation (the main objective of which is to assist N−H bond breaking).[23] This is at variance with expectations for a radical reaction mechanism, but confirms the validity of our thermodynamic analysis. Clearly, our investigation suggests that additional mass spectroscopy experiments should be performed for the TMG-NH_3 system, especially in higher molecular weight regions. Further experimental investigation in this direction is very desirable and is expected to be promising.

TABLE 4: Standard Enthalpies (kJ mol^{-1}) and Entropies (J mol^{-1} K^{-1}) for Dissociation Reactions (1) to (5) (See Left): B3LYP/PVDZ Level of Theory

process	ΔH^0_{298}	ΔS^0_{298}
(1)	215.3	337.1
(4)	179.8	531.5
(5)	71.8	470.2
(2)	287.0	481.4
(3)	179.0	420.1

Acknowledgment. A.Y.T. gratefully acknowledges financial support of the Center of Natural Science, Russia, Grants M98-2.5Π-485 and M99-2.5Π -160. H.F.B. is grateful to Prof. Dr. Sander and Prof. Dr. Scuseria for support. The work in Athens was supported by the National Science Foundation, Grant CHR-9815397. The authors thank Priv.-Doz. Dr. J. Müller (Ruhr-Universität Bochum) for reading the manuscript. We thank a referee for the helpful comments and for pointing out reference 57b to us.

Supporting Information Available: Harmonic vibrational frequencies and IR intensities for investigated compounds. This material is available free of charge via the Internet at http://pubs.acs.org.

References and Notes

(1) Thon, A.; Kuech, T. F. *Appl. Phys. Lett.* **1996**, *69*, 55.
(2) Bock, C. W.; Dobbs, K. D.; Mains, G. J.; Trachtman, M. *J. Phys. Chem.* **1991**, *95*, 7668.
(3) Graves, R. M.; Scuseria, G. E. *J. Chem. Phys.* **1992**, *96*, 3723.
(4) Bock, C. W.; Trachtman, M.; Mains, G. J. *J. Phys. Chem.* **1992**, *96*, 3007.
(5) Bock, C. W.; Trachtman, M. *J. Phys. Chem.* **1993**, *97*, 3183.

(6) Trachtman, M.; Beebe, S.; Bock, C. W. *J. Phys. Chem.* **1995**, *99*, 15028.
(7) Tirtowidjojo, M.; Pollard, R. *J. Cryst. Growth* **1988**, *93*, 108.
(8) Cui, S.; Hacker, D. K.; Xin, Q.-S.; Hinton, R. A.; Zhu, X.-Y. *J. Phys. Chem.* **1995**, *99*, 11515.
(9) Tanaka, H.; Komeno, J. *J. Cryst. Growth* **1988**, *93*, 115.
(10) See, for example: (a) Proceedings of the Sixth International Conference on Chemical Beam Epitaxy and Related Growth Techniques. *J. Cryst. Growth.* **1998**, *188*, 1−398. (b) Proceedings of the Ninth International Conference on Metalorganic Vapor Phase Epitaxy, La Jolla, California, USA. *J. Cryst. Growth* **1998**, *195*, 242−340. (c) Proceedings of the Tenth International Conference on Molecular Beam Epitaxy, Cannes, France. *J. Cryst. Growth* **1999**, *201*/*202*, 290−447.
(11) Kim, S. H.; Kim, H. S.; Hwang, J. S.; Choi, J. G.; Chong, P. J. *Chem. Mater.* **1994**, *6*, 278.
(12) Kawabata, T.; Matsuda, T.; Koike, S. *J. Appl. Phys.* **1984**, *56*, 2367.
(13) Safvi, S. A.; Redwing, J. M.; Tischler, M. A.; Kuech, T. F. *J. Electrochem. Soc.* **1997**, *144*, 1789.
(14) Neumayer, D. A.; Ekerdt, J. G. *Chem. Mater.* **1996**, *8*, 9.
(15) Timoshkin, A. Y.; Suvorov, A. V.; Bettinger, H. F.; Schaefer, H. F. *J. Am. Chem. Soc.* **1999**, *121*, 5687.
(16) Kim, H. J.; Egashira, Y.; Komiyama, H. *Appl. Phys. Lett.* **1991**, *59*, 2521.
(17) Egashira, Y.; Kim, H. J.; Komiyama, H. *J. Am. Ceram. Soc.* **1994**, *77*, 2009.
(18) Timoshkin, A. Y.; Bettinger, H. F.; Schaefer, H. F. *J. Am. Chem. Soc.* **1997**, *119*, 5668.
(19) *Gmelin Handbook of Inorganic Chemistry. Ga. Organogallium Compounds*; 8th ed.; Springer-Verlag: Berlin, 1987.
(20) Jennings, J. R.; Pattison, I.; Wade, K.; Wyatt, B. K. *J. Chem. Soc. A.* **1967**, 1608.
(21) Weller, F.; Dehnicke, K. *Chem. Ber.* **1977**, *110*, 3935.
(22) Almond, M. J.; Drew, M. G. B.; Jenkins, C. E.; Rice, D. A. *J. Chem. Soc. Dalt. Trans.* **1992**, 5.
(23) Demchuk, A.; Porter, J.; Koplitz, B. *J. Phys. Chem. A* **1998**, *102*, 8841.
(24) Lee, R. T.; Stringfellow, G. B. *J. Electron. Mater.* **1999**, *28*, 963.
(25) (a) Miehr, A.; Mattner, M. R.; Fischer, R. A. *Organometallics* **1996**, *15*, 2053. (b) Miehr, A.; Ambacher, O.; Rieger, W.; Metzger, T.; Born, E.; Fischer, R. A. *Chem. Vap. Deposition* **1996**, *2*, 51.
(26) Schäfer, J.; Simons, A.; Wolfrum, J.; Fischer, R. A. *Chem. Phys. Lett.* **2000**, *319*, 477.
(27) Ekerdt, J. G.; Sun, Y.-M.; Szabo, A.; Szulczewski, G. J.; White, J. M. *Chem. Rev.* **1996**, *96*, 1499.
(28) Gates, S. M. *Chem. Rev.* **1996**, *96*, 1519.
(29) Frisch, M. J.; Trucks, G. W.; Schlegel, H. B.; Gill, P. M. W.; Johnson, B. G.; Robb, M. A.; Cheeseman, J. R.; Keith, T.; Petersson, G. A.; Montgomery, J. A.; Raghavachari, K.; Al-Laham, M. A.; Zakrzewski, V. G.; Ortiz, J. V.; Foresman, J. B.; Cioslowski, J.; Stefanov, B. B.; Nanayakkara, A.; Challacombe, M.; Peng, C. Y.; Ayala, P. Y.; Chen, W.; Wong, M. W.; Andres, J. L.; Replogle, E. S.; Gomperts, R.; Martin, R. L.; Fox, D. J.; Binkley, J. S.; Defrees, D. J.; Barker, J.; Stewart, J. P.; Head-Gordon, M.; Gonzalez, C.; and Pople, J. A. GAUSSIAN 94, Revision C.3; Gaussian, Inc., Pittsburgh, PA, 1995.
(30) Becke, A. D. *J. Chem. Phys.* **1993**, *98*, 5648.
(31) Lee, C.; Yang, W.; Parr, R. G. *Phys. Rev. B.* **1988**, *37*, 785.
(32) a) Schäfer, A.; Horn, H.; Ahlrichs, R. *J. Chem. Phys.* **1992**, *97*, 2571. (b) Basis sets were obtained from the Extensible Computational Chemistry Environment Basis Set Database, as developed and distributed by the Molecular Science Computing Facility, Environmental and Molecular Sciences Laboratory, which is part of the Pacific Northwest Laboratory, P.O. Box 999, Richland, WA 99352, and funded by the, U.S. Department of Energy. The Pacific Northwest Laboratory is a multiprogram laboratory operated by Battelle Memorial Institue for the U.S. Department of Energy under Contract DE-AC06-76RLO 1830. Contact David Feller or Karen Schuchardt for further information.
(33) (a) Hay, P. J.; Wadt, W. R. *J. Chem. Phys.* **1985**, *82*, 270. (b) Wadt, W. R.; Hay P. J. *J. Chem. Phys.* **1985**, *82*, 284. (c) Hay, P. J.; Wadt, W. R. *J. Chem. Phys.* **1985**, *82*, 299.
(34) Campbell, J. P.; Hwang, J.-W.; Young, V. G.; Von Dreele, R. B.; Cramer, C. J.; Gladfelter, W. L. *J. Am. Chem. Soc.* **1998**, *120*, 521.
(35) Baxter, P. L.; Downs, A. J.; Rankin, D. W. H.; Robertson, H. E. *J. Chem. Soc., Dalton. Trans.* **1985**, 807.
(36) Greenwood, N. N.; Ross, E. J. F.; Storr, A. *J. Chem. Soc. A.* **1966**, 706.
(37) Veith, M. *Chem. Rev.* **1990**, 3.
(38) Downs, A. J., Ed. *Chemistry of Aluminum, Gallium, Indium and Thallium*; Chapman and Hall; New York, 1993.
(39) (a) Neumayer, D. A.; Cowley, A. H.; Decken, A.; Jones, R. A.; Lakhotia, V.; Ekerdt, J. G. *J. Am. Chem. Soc.* **1995**, *117*, 5893. (b) Neumayer, D. A.; Cowley, A. H.; Decken, A.; Jones, R. A.; Lakhotia, V.; Ekerdt, J. G. *Inorg. Chem.* **1995**, *34*, 4698.
(40) (a) Atwood, D. A.; Jones, R. A.; Cowley, A. H.; Atwood, J. L.; Bott, S. G. *J. Organomet. Chem.* **1990**, *394*, C6. (b) Atwood, D. A.; Atwood, V. O.; Cowley, A. H.; Jones, R. A.; Atwood, J. L.; Bott, S. G. *Inorg. Chem.* **1994**, *33*, 3251.
(41) Barry, S. T.; Richeson, D. S. *J. Organomet. Chem.* **1996**, *510*, 103.
(42) (a) Atwood, D. A.; Atwood, V. O.; Carriker, D. F.; Cowley, A. H.; Gabbai, F. P.; Jones, R. A.; Bond, M. R.; Carrano, C. J. *J. Organomet. Chem.* **1993**, *463*, 29. (b) Atwood, D. A.; Jones, R. A.; Cowley, A. H.; Bott, S. G.; Atwood, J. L. *Polyhedron* **1991**, *10*, 1897. (c) Atwood, D. A.; Jones, R. A.; Cowley, A. H.; Bott, S. G.; Atwood, J. L. *J. Organomet. Chem.* **1992**, *434*, 143. (d) Atwood, P. A.; Jones, R. A.; Cowley, A. H.; Bott, S. G.; Atwood, J. L. *Polyhedron* **1991**, *10*, 1897.
(43) Schauer, S. J.; Lake, C. H.; Watkins, C. L.; Krannich, L. K.; Powell, D. H. *J. Organomet. Chem.* **1997**, *549*, 31.
(44) Nutt, W. R.; Murray, K. J.; Gulick, J. M.; Odom, J. D.; Ding, Y.; Lebioda, L. *Organometallics*, **1996**, *15*, 1728.
(45) (a) Park, J. T.; Kim, Y.; Kim, J.; Kim, K.; Kim, Y. *Organometallics* **1992**, *11*, 3320. (b) Cho, D.; Park, J. E.; Bae, B.-J.; Lee, K.; Kim, B.; Park, J. T. *J. Organomet. Chem.* **1999**, *592*, 162. (c) Bae, B.-J.; Park, J. E.; Kim, Y.; Park, J. T.; Suh, I.-H. *Organometallics* **1999**, *18*, 2513.
(46) (a) Waggoner, K. M.; Power, P. P. *J. Am. Chem. Soc.* **1991**, *113*, 3385. (b) Waggoner, K. M.; Olmstead, M. M.; Power, P. P. *Polyhedron* **1990**, *9*, 257.
(47) Lee, B.; Pennington, W. T.; Robinson, G. H. *Inorg. Chim. Acta* **1991**, *190*, 173.
(48) (a) Beachley, O. T., Jr.; Noble, M. J.; Churchill, M. R.; Lake, C. H. *Organometallics* **1998**, *17*, 3311. (b) Beachley, O. T., Jr.; Noble, M. J.; Churchill, M. R.; Lake, C. H. *Organometallics* **1992**, *11*, 1051.
(49) (a) Jegier, J. A.; McKernan, S.; Gladfelter, W. L. *Inorg. Chem.* **1999**, *38*, 2726. (b) Jegier, J. A.; McKernan, S.; Gladfelter, W. L. *Chem. Mater.* **1998**, *10*, 2041.
(50) (a) Henderson, M. J.; Kennard, C. H. L.; Raston, C. L.; Smith, G. *J. Chem. Soc., Chem. Commun.* **1990**, 1203. (b) Janik, J. F.; Wells, R. L. *Inorg. Chem.* **1997**, *36*, 4135.
(51) Matsunaga, N.; Gordon, M. S. *J. Am. Chem. Soc.* **1994**, *116*, 11407.
(52) McDonald, T. R. R.; McDonald, W. S. *Proc. Chem. Soc.* **1962**, 366.
(53) Belgardt, T.; Roesky, H. W.; Noltemeyer, M.; Schmidt, H.-G. *Angew. Chem., Int. Ed. Engl.* **1993**, *32*, 1056.
(54) Belgardt, T.; Waezsada, S. D.; Roesky, H. W.; Gornitzka, H.; Häming, L.; Stalke, D. *Inorg. Chem.* **1994**, *33*, 6247.
(55) Cordeddu, F.; Hausen, H.-D.; Weidlein, J. *Z. Anorg. Allg. Chem.* **1996**, *622*, 573.
(56) Kühner, S.; Kuhnle, R.; Hausen, H.-D.; Weidlein, J. *Z. Anorg. Allg. Chem.* **1997**, *623*, 25.
(57) (a) Schnitter, C.; Waezsada, S. D:; Roesky, H. W.; Teichert, M.; Usón, I.; Parisini, E. *Organometallics* **1997**, *16*, 1197. (b) Schmid, K.; Niemeyer, M.; Weidlein, J. *Z. Anorg. Allg. Chem.* **1999**, *625*, 186.
(58) Nakamoto, K. *Infrared and Raman Spectra of Inorganic and Coordination Compounds*; 4th ed.; Wiley: New York, 1986.
(59) Durig, J. R.; Chatterjee, K. K. *J. Raman Spectrosc.* **1981**, *11*, 168.
(60) Greenwood, N. N.; Storr, A.; Wallbridge, M. G. H. *Inorg. Chem.* **1963**, *2*, 1036.
(61) Greenwood, N. N.; Storr, A.; Wallbridge, M. G. H. *Proc. Chem. Soc. London* **1962**, 249.
(62) Durig, J. R.; Bradley, C. B.; Li, Y. S.; Odom, J. D. *J. Mol. Struct.* **1981**, *74*, 205.
(63) Timoshkin, A. Y.; Bettinger, H. F.; Schaefer, H. F. *J. Phys. Chem. A.* **2001, *105***, 3240.